Dynamic States of V_2O_5 Supported on SnO_2/SiO_2 and CeO_2/SiO_2 Mixed-Oxide Catalysts during Methanol Oxidation

Jih-Mirn Jehng

Department of Chemical Engineering, National Chung Hsing University, Taichung 402, Taiwan, ROC

Received: January 5, 1998; In Final Form: April 20, 1998

A series of V_2O_5 supported on the SnO_2/SiO_2 and CeO_2/SiO_2 mixed oxides were investigated during methanol oxidation by in situ Raman spectroscopy, and the catalytic properties of these catalysts were probed by methanol oxidation kinetic studies. The Raman studies revealed that tin oxide forms a surface SnO_x overlayer on the silica surface owing to the absence of Raman features of the SnO_2 crystallite, but cerium oxide forms bulk CeO_2 particles on the silica surface. The impregnated vanadium oxide formed a surface vanadia overlayer on all the catalysts owing to the absence of V_2O_5 crystallite Raman features. In situ Raman studies of the $V_2O_5/SnO_2/SiO_2$ and $V_2O_5/CeO_2/SiO_2$ catalysts during methanol oxidation indicate that the formation of the VO_x-SnO_x and VO_x-CeO_2 interactions totally blocks the formation of surface $V-OCH_3$ groups, which are observed in the V_2O_5/SiO_2 catalysts. The interaction between the surface VO_x and the surface SnO_x overlayer on silica increases the methanol oxidation reactivity by 1−2 orders of magnitude relative to V_2O_5/SiO_2, and partial interaction between the surface VO_x and bulk CeO_2 particles increases the methanol oxidation reactivity by 0−1 order of magnitude relative to V_2O_5/SiO_2. Temperature programmed reduction (TPR) studies indicate that the reducibility of the surface vanadium oxide species is dependent on the reducibility of the specific oxide support and confirm the formation of the VO_x-SnO_x bonds for the $V_2O_5/SnO_2/SiO_2$ catalyst and the formation of VO_x-CeO_2 as well as VO_x-SiO_2 bonds for the $V_2O_5/CeO_2/SiO_2$ catalyst.

Introduction

Recent studies of V_2O_5 supported on TiO_2/SiO_2 catalysts have demonstrated that the presence of TiO_2 on the SiO_2 surface decreases the reduction temperature of the supported vanadia phase and that these mixed-oxide systems exhibit a high reactivity for the selective catalytic reduction (SCR) of NO with NH_3 relative to the V_2O_5/SiO_2 system.[1−6] The use of a SiO_2 support for the V_2O_5/TiO_2 catalysts for the reduction of NO_x with NH_3 results in a higher surface area, superior sintering resistance, and low cost compared with the use of a TiO_2 support.[5,7] In addition, the formation of a surface TiO_x overlayer between the surface VO_x and the SiO_2 support increases the TOF (turnover frequency) for methanol oxidation by 2 orders of magnitude relative to the V_2O_5/SiO_2 system owing to the presence of the VO_x-TiO_x surface interactions.[8] The catalytic studies of the $V_2O_5/TiO_2/SiO_2$ catalysts suggest that the surface VO_x-TiO_x interactions are more pronounced than the surface VO_x-SiO_2 interactions and strongly affect the reactivity of the surface vanadia species.[9]

The V_2O_5 supported on SnO_2 and CeO_2 catalysts are often used for the application of hydrocarbon oxidation reactions.[10,11] The molecular structures of the V_2O_5 supported on SnO_2 and CeO_2 catalysts were recently investigated by solid-state ^{51}V and ^1H NMR, electron spin resonance, and in situ Raman techniques.[11−16] The solid-state ^{51}V and ^1H NMR results indicated the formation of a surface vanadia overlayer on SnO_2 with a monolayer coverage of 3.2 wt % V_2O_5.[11−13] The ESR results indicated that the reduced V_2O_5/SnO_2 catalysts form an isolated V^{4+} (or VO^{2+}) species in a distorted oxygen environment.[11,14,15] In situ Raman studies revealed that the dehydrated surface vanadia species on the SnO_2 support possess Raman bands at ∼1027, ∼900, and ∼830 cm^{-1} [16] and that the dehydrated surface vanadium oxide species on the CeO_2 support possess Raman bands at ∼1027 and ∼920 cm^{-1}. Consequently, the dehydrated surface vanadia species with a terminal V═O (Raman band at ∼1027 cm^{-1}) and surface polymeric vanadate functionalities (Raman band in the 900−920 cm^{-1} region) exist on both the SnO_2 and CeO_2 surfaces. However, the dehydrated V_2O_5/SiO_2 catalyst only posesses a single Raman band at ∼1038 cm^{-1}. The dehydrate surface vanadium oxide species, which give rise to the sharp Raman bands in the 1027−1038 cm^{-1} region, also exhibit IR bands in the 1020−1040 cm^{-1} region.[17] The coincidence of the IR and Raman bands suggests that isolated surface vanadia species containing one terminal V═O bond and three bridging V−O−Si bonds are present.[9,17−20] The corresponding solid-state ^{51}V NMR shift appears at ∼640 ppm, which is consistent with tetrahedral coordination.[21,22] In situ XANES/EXAFS studies on V_2O_5 supported on SiO_2 catalysts also suggest that the surface vanadia species on SiO_2 possess an isolated mono-oxo tetrahedral vanadate structure.[23] From this structural characterization information, the sharp Raman band in the 1027−1038 cm^{-1} has been assigned to the isolated vanadate species possessing one terminal V═O bond and three bridging V−O support bonds.[24−30] The broad Raman band in the 900−920 cm^{-1} region has been assigned to polymeric tetrahedral metavanadate species.[27,29,30] However, the polymeric vanadate species also possess a V═O terminal bond at 1027−1038 cm^{-1}, which is overlapping with the isolated vanadate species.

The reactivity of the methanol oxidation reaction over the V_2O_5/SnO_2 and V_2O_5/CeO_2 catalysts is higher than that of the V_2O_5/TiO_2 catalyst, and the presence of redox sites on the V_2O_5/SnO_2 and V_2O_5/CeO_2 catalysts results in the high selectivity of HCHO, $HCOOCH_3$, and $(CH_3O)_2CH_2$. In addition, in situ

S1089-5647(98)00622-1 CCC: $15.00
Published on Web 07/08/1998

Raman studies of the V_2O_5/SnO_2 catalyst for methane activation reaction indicated that the surface vanadia species on SnO_2 can be easily reduced with the presence of methane.[16] The high reactivity of methanol partial oxidation over the V_2O_5/SnO_2 catalysts was also observed by Reddy et al.[28] Thus, it is possible that the $V_2O_5/SnO_2/SiO_2$ and $V_2O_5/CeO_2/SiO_2$ catalysts can be developed and that they will exhibit activities higher than those of the $V_2O_5/TiO_2/SiO_2$ catalysts.

In this study, the molecular structures of V_2O_5 supported on SnO_2/SiO_2 and CeO_2/SiO_2 catalysts during methanol oxidation reaction will be studied by in situ Raman spectroscopy. The reducibility of these mixed metal oxide catalysts will be investigated by temperature programmed reduction (TPR) in order to determine the interaction between the surface vanadia species and the mixed-oxide support. The catalytic properties of these catalysts will be probed by the methanol oxidation reaction. Combing the structural information and the catalytic studies will provide a better understanding of the surface active sites of these mixed metal oxide systems.

Experimental Section

a. Materials and Preparation. The V_2O_5 supported on the SnO_2/SiO_2 and CeO_2/SiO_2 mixed oxides were prepared by the incipient-wetness impregnation method. The SiO_2 (Cab-O-Sil, EH 5, ~380 m^2/g) support was pretreated with water and calcined at 500 °C for 16 h under flowing dry air in order to condense its volume. The water pretreated procedure has no effect on the BET surface area of the silica support. For the SnO_2/SiO_2 mixed-oxide support, tin isopropoxide (Alfa, 15% in propanol) in a propanol solution (Fisher, HPLC grade) was impregnated in the silica support under a nitrogen environment. The samples were initially dried at room temperature for 2 h to remove excess propanol and further dried at 120 °C for 16 h under flowing N_2. The samples were finally calcined at 500 °C for 1 h under flowing N_2 and for an additional 15 h under flowing dry air. Multiple impregnation steps were used to prepare the 30% SnO_2/SiO_2 mixed-oxide support. For the CeO_2/SiO_2 mixed-oxide support, cerium nitrate in aqueous solution was used to impregnate the silica support. The samples were initially dried at 120 °C for 16 h and further calcined at 500 °C for 16 h under flowing dry air. Vanadium isopropoxide (Alfa, 95−99% purity) in a methanol solution (Fisher, 99.9% purity) was impregnated in the SnO_2/SiO_2 and CeO_2/SiO_2 supports by using the same nonaqueous preparation procedures as for the SnO_2/SiO_2 system.

b. In Situ Raman Spectroscopy. The in situ Raman spectrometer system consists of a quartz cell and a sample holder, a triple-grating spectrometer (Spex, model 1877), a photodiode array detector (EG&G, Princeton Applied Research, model 1420), and an argon ion laser (Spectra-Physics, model 165). The sample holder is made from a metal alloy (Hastalloy C), and a 100−200 mg sample disk is held by the cap of the sample holder. The sample holder is mounted onto a ceramic shaft that is rotated by a 115 V dc motor at a speed of 1000−2000 rpm. A cylindrical heating coil surrounding the quartz cell is used to heat the cell. The quartz cell is capable of operating up to 600 °C, and flowing gas is introduced into the cell at a rate of 100−300 cm^3/min at atmospheric pressure.

The in situ Raman spectra were obtained in the following procedures. The samples were placed in the cell and heated to 500 °C for 1 h in a flow of pure oxygen gas (Linde Specialty Grade, 99.99% purity). The dehydrated Raman spectra were collected after cooling the sample to 230 °C in a flow of pure oxygen gas for 30 min. After the above treatment, a gaseous mixture with an He/O_2 ratio near $^{11}/_6$ containing saturated methanol vapor in an ice bath (~4 mol % CH_3OH) was introduced into the cell, and the Raman spectra under reaction conditions were collected after a steady state was reached. Raman features of the surface vanadia species appear in the 100−1200 cm^{-1} region, and the surface methoxy (CH_3O− species) appear in the 2750−3100 cm^{-1} region.

c. Temperature Programmed Reduction Experiment. A thermal gravimetric/differential thermal analysis (TG/DTA) system (SEIKO model 220) was used to study the reduction characteristic of the V_2O_5 supported on SnO_2/SiO_2 and CeO_2/SiO_2 catalysts. The sample was first treated to 500 °C with a 20 °C/min heating rate under a flowing nitrogen (50−200 cm^3/min) and oxygen (50 cm^3/min) mixture gas and maintained at 500 °C for 1 h in order to remove the adsorbed moisture and oxidize the catalysts. The sample was then cooled to room temperature and maintained at room temperature for 30 min. Then the treatment gas was switched to a 5% H_2 balance in He gas with a 50 cm^3/min flow rate. The sample was heated with a 20 °C/min heating rate to a final temperature of 800−1000 °C. Typically, various runs were carried out on a particular sample by decreasing the sample weight in order to observe similar reduction profiles and to eliminate error due to mass and heat transfer. The weight of the samples corresponding to 0.1−2.4 mg of V_2O_5 was used for the TPR studies. The weight of the sample was obtained as a function of time, and for the reduction cycle the rate of change of sample weight per unit time was also obtained. This also provides the rate of sample weight per unit temperature change, dW/dT, since the ramp rate during the reduction cycle is linear. The temperature where the maximum value of dW/dT occurred is denoted as $T_{max.}$

d. Methanol Oxidation Studies. The catalytic properties of the V_2O_5 supported on SnO_2/SiO_2 and CeO_2/SiO_2 catalysts were probed with the sensitive methanol reaction in order to determine the relative reactivity of these catalysts. The catalytic reactor consisted of a digital flow rate controller (Brooks), a tube furnace (Lindberg), a condenser and methanol reservoir, and an on-line gas chromatograph (HP 5890 series II). A mixture of He and O_2 gases was flowed through the methanol reservoir with the condenser maintained at 9.6 °C. The methanol concentration in the feed gas was obtained by calculating the partial pressure of methanol at this temperature. The 6.2:13:80.8 proportion of the $CH_3OH/O_2/He$ gaseous mixture then flowed to the reactor. The catalysts were placed in the center of a 6 mm o.d. Pyrex microreactor supported by quartz wool, and activated at 500 °C under flowing pure oxygen gas. The reactor was then cooled to the 230 °C reaction temperature. The effluent gas was analyzed by gas chromatography. The catalytic activity and selectivity were obtained by integrating the peak areas of the products with respect to the reference peak area of methanol. The methanol conversion was kept below 10% to avoid complications due to the heat and mass limitations.

Results

a. Raman Spectroscopy. *In Situ Raman Spectra under Dehydrated Conditions.* The dehydrated Raman spectra of the 1−3% V_2O_5 supported on SnO_2/SiO_2 and CeO_2/SiO_2 catalysts are shown in Figures 1 and 2. The Raman results suggest that the surface SnO_x species is present on the dehydrated 1−3% V_2O_5 supported on 3% SnO_2/SiO_2 and 30% SnO_2/SiO_2 catalysts owing to the absence of Raman features of SnO_2 crystallites (Raman bands at ~750, ~622 (s), ~500, ~320, and ~240 cm^{-1}) (see Figure 1), but bulk CeO_2 (Raman bands at ~600, ~455,

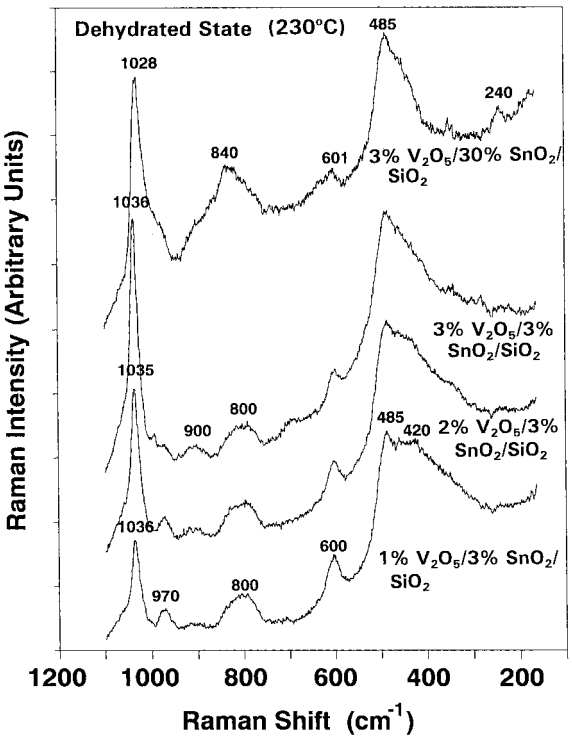

Figure 1. Dehydrated Raman spectra of the V_2O_5 supported on SnO_2/SiO_2 as a function of V_2O_5 and SnO_2 loading.

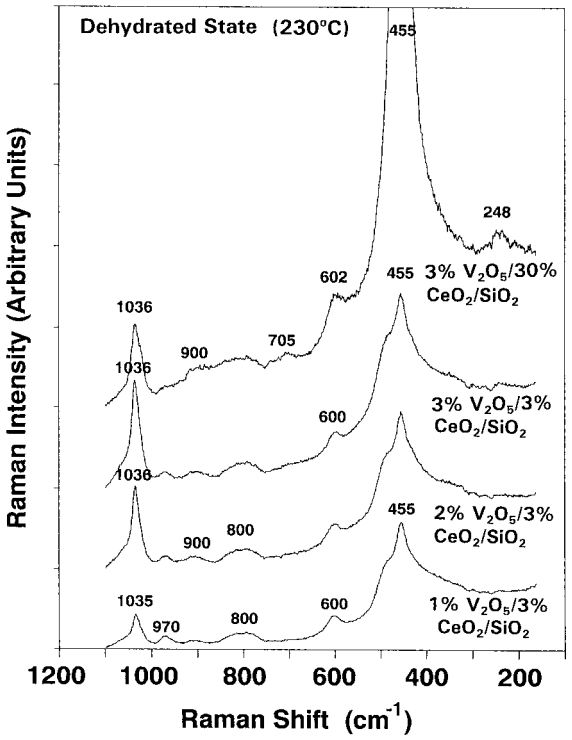

Figure 2. Dehydrated Raman spectra of the V_2O_5 supported on CeO_2/SiO_2 as a function of V_2O_5 and CeO_2 loading.

and ~240 cm^{-1}) is present on all the $V_2O_5/CeO_2/SiO_2$ catalysts (see Figure 2). No crystalline V_2O_5 features (major Raman bands at ~994, ~702, ~527, ~404, ~284, and ~146 cm^{-1}) are observed in the sample.[31] The similar Raman band at ~1035 cm^{-1} for the $V_2O_5/3\%$ SnO_2/SiO_2 and $V_2O_5/3\%$ CeO_2/SiO_2 catalysts compared with those of the V_2O_5/SiO_2 catalysts indicates that vanadium oxide preferentially interacts with the silica surface to form an isolated VO_4 species with one terminal V═O bond. The shift of the dehydrated vanadia species was

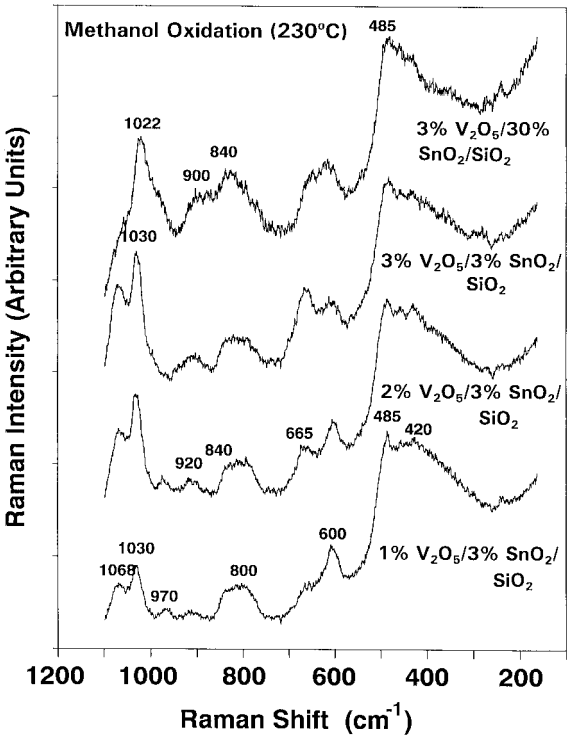

Figure 3. In situ Raman spectra of the V_2O_5 supported on SnO_2/SiO_2 as a function of V_2O_5 and SnO_2 loading during methanol oxidation in the 100−1200 cm^{-1} region.

from ~1035 to ~1028 cm^{-1} (see Figure 1), and the appearance of the broad Raman bands was in the 850−950 cm^{-1} region for the 3% $V_2O_5/30\%$ SnO_2/SiO_2 catalyst, which are similar to Raman features of the V_2O_5/SnO_2 catalyst.[16] The broadening of the Raman band at ~1036 cm^{-1} (see Figure 2) and the broad and weak Raman band in the 850−950 cm^{-1} region are observed for the 3% $V_2O_5/30\%$ CeO_2/SiO_2 catalyst.

In Situ Raman Spectra during Methanol Oxidation. Previous in situ Raman studies of the pure silica support during methanol oxidation have shown that methanol molecules partially react with the surface silanol groups to form a surface methoxy species.[32−34] The surface methoxy groups possess Raman bands at ~2956 and ~2856 cm^{-1} that are characteristic of the C−H symmetric stretching vibration and a weak Raman band at 2990 cm^{-1} that is characteristic of the C−H asymmetric stretching vibration.[32,33]

The in situ Raman spectra of the 1−3% V_2O_5 supported on SnO_2/SiO_2 and CeO_2/SiO_2 during methanol reaction are shown in Figures 3−6. The Raman intensity of the dehydrated surface vanadia species (1028−1036 cm^{-1}) decreases, and the band shifts ~5−8 cm^{-1} toward lower wavenumber, and additional Raman bands appear at ~1068 and ~665 cm^{-1} (see Figures 3 and 5). Raman bands at ~1068 and ~665 cm^{-1} are associated with vanadium alkoxide compounds and have been assigned to terminal V═O and bridging V−O−R vibrations, respectively.[32,35] At low loading of SnO_2 and CeO_2 (3%), Raman bands at ~2957, ~2933, ~2858, and ~2835 cm^{-1} appear and the intensities of the two Raman bands at ~2933 and ~2835 cm^{-1} increase with increasing surface vanadia loading (see Figures 4 and 6). The intensities of the ~2933 and ~2835 cm^{-1} Raman bands decreased with increasing SnO_2 and CeO_2 loading to 30%. No Raman bands at ~2957 and ~2857 cm^{-1} are observed for the 3% $V_2O_5/30\%$ SnO_2/SiO_2 and 3% $V_2O_5/30\%$ CeO_2/SiO_2 catalyst.

b. Temperature Programmed Reduction (TPR). *TPR Studies of V_2O_5 Supported on Pure Oxide Supports.* TPR results

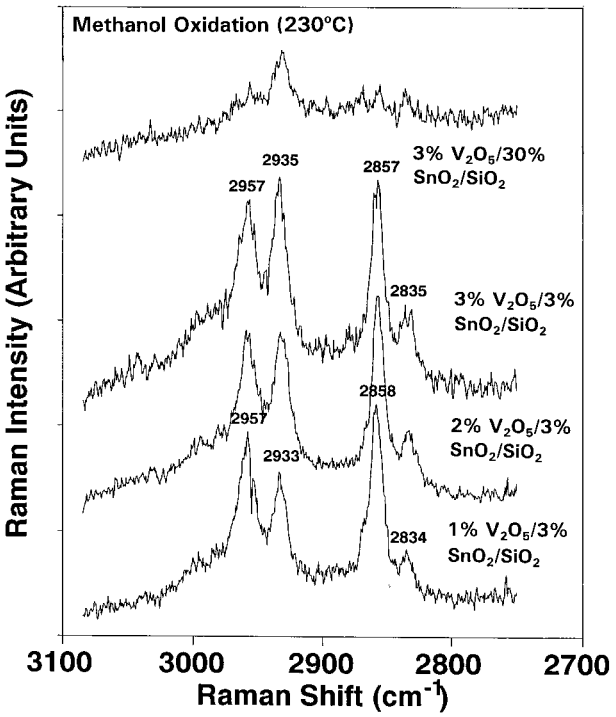

Figure 4. In situ Raman spectra of the V_2O_5 supported on SnO_2/SiO_2 as a function of V_2O_5 and SnO_2 loading during methanol oxidation in the 2700−3100 cm^{-1} region.

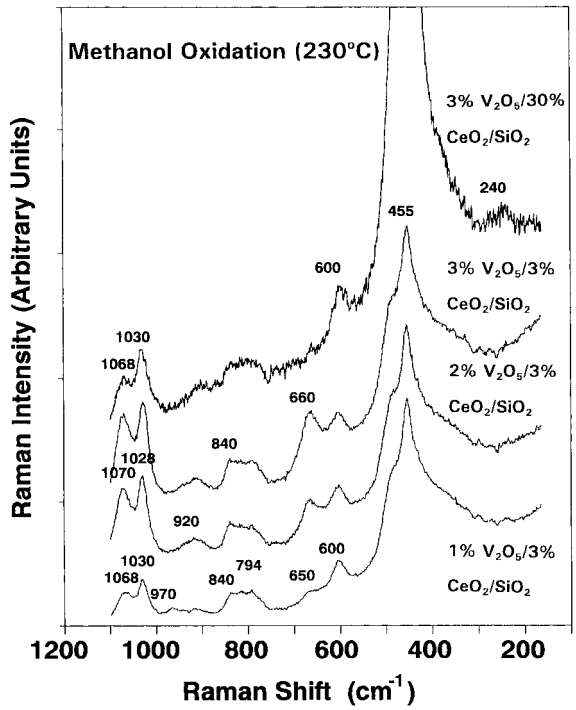

Figure 5. In situ Raman spectra of the V_2O_5 supported on CeO_2/SiO_2 as a function of V_2O_5 and CeO_2 loading during methanol oxidation in the 100−1200 cm^{-1} region.

for V_2O_5 supported on different oxide supports (such as SnO_2, CeO_2, TiO_2, and SiO_2) are shown in Table 1. The TPR studies indicate that the T_{max} position is strongly dependent on the specific oxide support. The 7% V_2O_5/SiO_2 catalyst possesses only one T_{max} peak at ∼660 °C, and the V_2O_5/TiO_2 catalyst possesses two T_{max} peaks at ∼550 and ∼593 °C. Three T_{max} peaks appear at ∼580, ∼635, and ∼745 °C for the V_2O_5/CeO_2 catalyst and at ∼460, ∼570, and ∼715 °C for the V_2O_5/SnO_2 catalyst. The highest reduction peak at ∼715 °C for the V_2O_5/SnO_2 catalyst and at ∼745 °C for the V_2O_5/CeO_2 catalyst is probably due to the reduction of the SnO_2 and CeO_2 supports or the formation of V−Sn−O and V−Ce−O solid solutions at high temperatures. The reducibility of the surface vanadium oxide on the various oxide supports has the following order: $V_2O_5/SnO_2 > V_2O_5/TiO_2 > V_2O_5/CeO_2 > V_2O_5/SiO_2$.

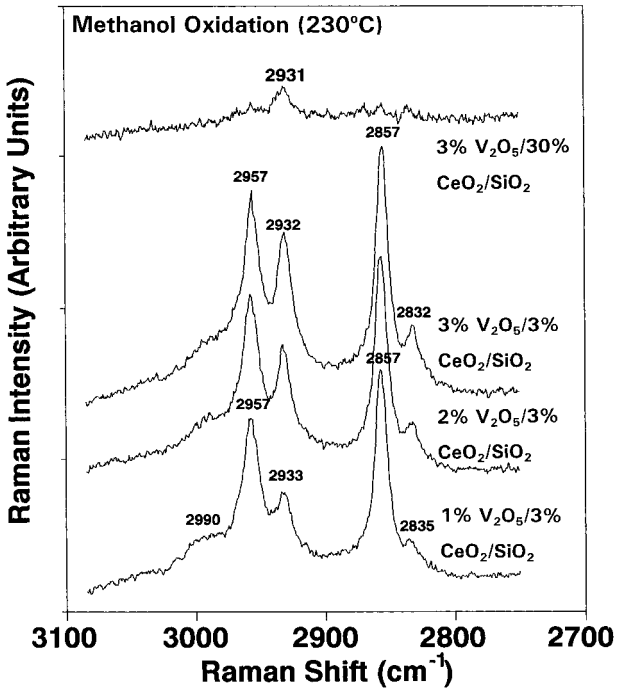

Figure 6. In situ Raman spectra of the V_2O_5 supported on CeO_2/SiO_2 as a function of V_2O_5 and CeO_2 loading during methanol oxidation in the 2700−3100 cm^{-1} region.

TABLE 1: Maximum Reduction Temperatures of Supported Vanadium Oxide on Pure Oxide Supports

catalysts	T_{max} (°C)
7% V_2O_5/SiO_2	660
5% V_2O_5/TiO_2	550, 593
3% V_2O_5/CeO_2	580, 635, 745
3% V_2O_5/SnO_2	460, 570, 715

TABLE 2: Maximum Reduction Temperatures of SiO_2, SnO_2/SiO_2, and Supported V_2O_5 on SnO_2/SiO_2

catalysts	T_{max} (°C)
SiO_2	
3% SnO_2/SiO_2	564
30% SnO_2/SiO_2	302, 517, 693
3% V_2O_5/3% SnO_2/SiO_2	653
3% V_2O_5/30% SnO_2/SiO_2	351, 526, 714, 758, 852

TPR Studies of V_2O_5 Supported on Mixed Oxide Supports. TPR studies of the V_2O_5 supported on SnO_2/SiO_2 catalysts are shown in Table 2 as a function of SnO_2 loading. No reduction peak occurs for the pure silica support. Upon the addition of 3% SnO_2 on silica, a weak and broad T_{max} peak is present at ∼564 °C, which is characteristic of the reduction of the surface tin oxide species. Additional T_{max} peaks at ∼320, ∼517, and ∼693 °C appear upon increasing the SnO_2 loading to 30%. The impregnation of 3% V_2O_5 on 3% SnO_2/SiO_2 exhibits a T_{max} peak at ∼653 °C, which is similar to the reduction peak of the V_2O_5/SiO_2 catalyst. At high loading of tin oxide (30%), multiple reduction peaks at ∼351, ∼526, ∼714, ∼758, and ∼852 °C, which indicates that vanadium oxide preferentially reacts with the surface tin oxide species to form a VO_x-SnO_x interaction. Multiple T_{max} peaks are characteristic of the reduction of both the surface vanadium oxide and tin oxide species.

TABLE 3: Maximum Reduction Temperatures of SiO_2, CeO_2/SiO_2, and Supported V_2O_5 on CeO_2/SiO_2

catalysts	T_{max} (°C)
SiO_2	
3% CeO_2/SiO_2	640
30% CeO_2/SiO_2	658, 852
3% V_2O_5/3% CeO_2/SiO_2	647
3% V_2O_5/30% CeO_2/SiO_2	501, 651, 852

TABLE 4: Catalysis of Methanol Oxidation Reaction over Supported Vanadium Oxide Catalysts

catalysts	activity ($\times 10^{-3}$)	TON (s^{-1})	selectivity[a] FM	MF	DMM	CO/CO_2
1% V_2O_5/TiO_2	59.4	1.5×10^{-1}	89.7	5.7	4.6	
1% V_2O_5/SnO_2	298.0	7.5×10^{-1}	69	19	2	10
3% V_2O_5/SnO_2	534.4	4.5×10^{-1}	85.7	3.2	11.1	
1% V_2O_5/CeO_2	99.0	2.5×10^{-1}	86.4	4.1	9.5	
3% V_2O_5/SiO_2	0.95	8.0×10^{-4} [b]				
30% SnO_2/SiO_2	19.3	2.7×10^{-3} [b]	100			
30% CeO_2/SiO_2	2.2	3.5×10^{-4} [c]				
3% V_2O_5/3% SnO_2/SiO_2	24.9	2.1×10^{-2}	82.1	11.9	6.0	
3% V_2O_5/3% CeO_2/SiO_2	2.7	2.3×10^{-3}	83.7	9.3	7.0	
3% V_2O_5/30% SnO_2/SiO_2	213.7	1.8×10^{-1}	86.8	11.5	1.7	
3% V_2O_5/30% CeO_2/SiO_2	29.7	2.5×10^{-2}	84.6	8.3	8.1	

[a] FM: HCHO. MF: $HCOOCH_3$. DMM: $(CH_3O)_2CH_2$. Activity: mole of CH_3OH converted per gram of catalyst per hour. TON: number of CH_3OH molecules converted per V atom per second. [b] TON based on Sn atom. [c] TON based on Ce atom.

TPR studies of the V_2O_5 supported on CeO_2/SiO_2 are shown in Table 3 as a function CeO_2 loading. The T_{max} peaks in the 647−651 °C region, which are similar to the reduction peak of the V_2O_5/SiO_2 catalyst, are observed on the $V_2O_5/CeO_2/SiO_2$ catalysts. This indicates that the surface vanadium oxide species preferentially reacts with the silica support to form a VO_x−SiO_2 interaction due to the poor dispersion of CeO_2. However, the reduction peak of the VO_x−CeO_2 interaction is difficult to identify because of the broad feature of this reduction peak.

c. Methanol Oxidation Studies. The catalytic properties of the V_2O_5 supported on various oxide supports during methanol oxidation at 230 °C reaction temperature are listed in Table 4. Catalytic studies of these catalysts reveal that the reactivity of the V_2O_5 supported on TiO_2 catalyst (89.7% HCHO selectivity) is 1−2 orders of magnitude higher than that of V_2O_5 supported on the SiO_2 catalyst (see Table 4). The reactivity of the V_2O_5 supported on SnO_2 and CeO_2 catalysts is 2−5 times higher than that of the V_2O_5 supported on TiO_2 catalyst. The surface tin oxide overlayer on the silica support enhances the reactivity of methanol oxidation relative to the pure silica support, which is essentially inactive for methanol oxidation (see Table 4). The impregnation of 3% V_2O_5 supported on 3% SnO_2/SiO_2 and 30% SnO_2/SiO_2 catalysts increases the methanol oxidation activity of these catalysts by 1−2 orders of magnitude relative to that of the 3% V_2O_5/SiO_2 catalyst. In addition, the HCHO selectivity increases from 0 to 82−87% upon the impregnation of 3% V_2O_5 on SnO_2/SiO_2 and CeO_2/SiO_2 mixed-oxide supports. The 3% V_2O_5 supported on 3% CeO_2/SiO_2 and 30% CeO_2/SiO_2 catalysts containing bulk CeO_2 particles exhibit methanol oxidation activity between the V_2O_5/SiO_2 and V_2O_5/CeO_2 catalysts.

Discussion

The structural characterization of the V_2O_5 supported on SnO_2/SiO_2 catalysts has revealed that the deposition of vanadium oxide and tin oxide on the SiO_2 support results in a two-dimensional surface vanadia and tin oxide overlayer due to the absence of crystalline V_2O_5 and SnO_2, respectively (see Figure 1).[16,31] The deposition of vanadium oxide on the CeO_2/SiO_2 supports also results in the formation of a surface vanadia overlayer; however, bulk CeO_2 particles are observed in the $V_2O_5/CeO_2/SiO_2$ catalysts (see Figure 2).

For the V_2O_5 supported on mixed-oxide catalysts with low SnO_2 and CeO_2 loading, a strong and sharp Raman band appearing at ∼1036 cm^{-1}, which is similar to the Raman features of the V_2O_5/SiO_2 catalyst, suggests that vanadium oxide preferentially interacts with the SiO_2 surface to form a surface vanadia phase possessing a mono-oxo VO_4 structure.[24−27] For the 3% V_2O_5/30% SnO_2/SiO_2 catalyst, the Raman shift of the dehydrated vanadia species from ∼1036 to ∼1028 cm^{-1} and the appearance of the broad and weak Raman bands in the 850−950 cm^{-1} region indicate that the isolated surface vanadia species and polymeric surface vanadate species coexist on the surface.[30,36,37] This is similar to the Raman features of the V_2O_5/SnO_2 catalyst[16] and suggests that the surface VO_x species preferentially interact with surface SnO_x species, since the silica surface has been mostly covered by the surface SnO_x species. The additional Raman band at ∼840 cm^{-1} is probably characteristic of the formation of a V−Sn−O solid solution in the $V_2O_5/SnO_2/SiO_2$ catalyst with high SnO_2 loading, since the position of this band is not affected by the dehydration treatments to remove the surface moisture and the presence of methanol molecules. The studies by Okada et al.[10] and Andersson[38] of the V_2O_5−SnO_2 catalysts indicated that a V−Sn−O solid solution was expected to form at higher SnO_2 concentration. The formation of a V−Sn−O complex on zeolite can inhibit the formation of V−zeolite interactions and can preserve the zeolite activity in catalytic cracking reactions.[39] The appearance of a strong Raman band at ∼1036 cm^{-1} for the 3% V_2O_5/30% CeO_2/SiO_2 catalyst indicates that the surface VO_x species mostly interact with the SiO_2 surface owing to the poor dispersion of cerium oxide on SiO_2 and the formation of bulk CeO_2 particles.

Previous in situ Raman studies of the V_2O_5/SiO_2 catalysts during methanol oxidation revealed that the terminal V═O Raman band at ∼1036 cm^{-1} generally decreased in intensity and shifted 5−10 cm^{-1} toward lower wavenumber.[32] These changes reflect the presence of adsorbed methoxy species on the catalyst surface, and the shift to lower wavenumber may be due to hydrogen bonding of the terminal V═O bonds with the surface methoxy species. In addition, surface Si−OCH_3 species with Raman bands at ∼2856 and ∼2958 cm^{-1} were formed by the interaction of the available surface Si−OH sites with methanol molecules,[33] and the surface vanadium oxide species were found to form stable V−OCH_3 complexes (Raman bands at ∼1070 and ∼665 cm^{-1}).[32] Additional strong surface methoxy Raman vibrations at ∼2932 and ∼2830 cm^{-1} have been assigned to the formation of surface V−OCH_3 species with corresponding V═O and V−O−R Raman bands at ∼1070 and ∼665 cm^{-1}. The stability of the surface V−OCH_3 complexes results in a low catalytic activity for the V_2O_5/SiO_2 system (see Table 1).

During methanol oxidation, the formation of the surface Si−OCH_3 species at ∼2856 and ∼2958 cm^{-1} due to the interaction of the available surface Si−OH sites with the methanol molecules was observed in the V_2O_5 supported on 3%SnO_2/SiO_2 and 3% CeO_2/SiO_2 catalysts (see Figures 3 and 5). In addition, the Raman intensities of the surface V−OCH_3 species at ∼2932 and ∼2830 cm^{-1} increased with increasing V_2O_5 loading (see Figures 4 and 6). However, in situ Raman studies of the 3% V_2O_5/30% SnO_2/SiO_2 catalyst during methanol oxidation indicate that the Raman band at ∼1028 cm^{-1} for the

terminal V=0 bonds decreased its intensity and shifted ~6 cm^{-1} toward lower wavenumber owing to the partially reduced surface vanadium oxide species and hydrogen bonding with the surface methoxy species (see Figure 3).[32] The absence of the Raman bands at ~2957 and ~2857 cm^{-1} in the 3% V_2O_5/30% SnO_2/SiO_2 catalyst indicates that surface SnO_x species are well-dispersed on the silica surface and that essentially no surface Si−OH sites are available for methanol molecules to form the surface Si−OCH_3 species (see Figure 4). According to XRD results, SnO_2 possesses a tetragonal rutile structure with a unit area of ~15.1×10^{-20} m^2, and a theoretical monolayer coverage of SnO_2 on SiO_2 (with a surface area of ~380 m^2/g) is calculated to be ~38.6%.[40] It appears that the surface VO_x species mainly anchor on the surface SnO_x species to form a VO_x-SnO_x interaction for the 3% V_2O_5/30% SnO_2/SiO_2 catalyst. The interactions between the surface vanadium oxide species and the SnO_2/SiO_2 and CeO_2/SiO_2 mixed-oxide supports can be further discriminated by the TPR and catalytic studies.

TPR experiments were used to study the reducibility of the surface vanadium oxide species as a function of oxide support (see Table 1). It appears that the reducibility of the surface vanadium oxide species is dependent on the reducibility of the oxide supports.[18,41−45] The SnO_2 and CeO_2 supports are reducible oxides, but the TiO_2 and SiO_2 supports, however, are not easily reducible. A decrease in the reduction peak results in a corresponding increase in the reactivity of the supported vanadium oxide catalysts, and the V−O−support bridging bond controls the reactivity and reducibility of the supported vanadium oxide catalysts.[41,42] Relating the reduction peak and the structural characterization of the V_2O_5 supported on pure oxide supports suggests that surface vanadium oxide on silica is only present as an isolated surface VO_4 species with a corresponding T_{max} peak at ~660 °C, and surface vanadium oxide on titania, cerium oxide, and tin oxide is present as both isolated vanadium oxide and polymeric vanadate species with two T_{max} peaks below ~660 °C (see Table 1).[46−48] This is consistent with the recent high-resolution TPR study of the supported vanadia catalysts in which the presence of two reduction peaks for the surface vanadia species reflected the coexistence of the isolated vanadia and polymeric vanadate species on the catalyst's surface.[45,46] In situ Raman studies of the reduction of the V_2O_5/TiO_2 catalyst, under ammonia or butane environments, demonstrated that the polymeric vanadia species are more easily reducible than the isolated vanadia species.[49,50] However, both isolated and polymeric surface vanadia species were equally reduced under hydrogen environment.[48]

The TPR studies of the V_2O_5 supported on pure oxide supports (such as SiO_2, TiO_2, CeO_2, and SnO_2) can be used as a reference to determine the reducibility and interaction of the surface vanadium oxide species on the SnO_2/SiO_2 and CeO_2/SiO_2 mixed-oxide supports. The formation of a surface SnO_x or CeO_2 overlayer on silica can influence the interactions of the surface vanadium oxide species and oxide support. At low SnO_2 (or CeO_2) loading, the VO_x-SiO_2 interactions are predominately formed on the surface owing to the presence of T_{max} in the 647−653 °C region, which is similar to the reduction peak of the V_2O_5/SiO_2 catalyst (see Tables 1 and 2). This is consistent with the Raman's structural characterization that the surface vanadia species only possess a mono-oxo VO_4 structure. At high SnO_2 loading, the presence of multiple T_{max} peaks at ~351, ~528, ~714, and ~758 °C are due to the reduction of surface vanadium oxide species and surface tin oxide species. It is difficult to discriminate these reduction peaks from its corresponding structure because of the overlapping of the reduction peaks of the VO_x and SnO_x species (see Table 2). However, the shift of the reduction peaks and the presence of new reduction peaks, compared with those of the V_2O_5/SnO_2 and SnO_2/SiO_2 systems, in the 3% V_2O_5/30% SnO_2/SiO_2 catalyst suggest that the VO_x-SnO_x interactions are formed on the silica surface. The absence of the reduction peak at ~660 °C indicates that the VO_x-SiO_2 interactions are not formed on the surface. The highest reduction peak at ~852 °C may be due to the presence of the V−Sn−O solid solution, which possesses a lower reducibility compared to the surface VO_x and SnO_x species.[43] Thus, the reducibility of the supported vanadium oxide catalysts is strongly dependent on the nature and the composition of the support. The formation of VO_x-SnO_x interactions on the V_2O_5/SnO_2/SiO_2 catalyst will be further discussed in the catalytic studies.

The catalytic properties of the V_2O_5 supported on the SnO_2/SiO_2 and CeO_2/SiO_2 catalysts were probed with the sensitive methanol oxidation reaction. The advantages of this probe reaction are that it is a simple reaction, and the reaction pathways are well-known in order to distinguish the different surface active sites that are present on the catalyst surface. The high selectivity of HCHO, $HCOOCH_3$, and $(CH_3O)_2CH_2$ over these catalysts reveals that redox sites are predominant on the surfaces of these catalysts (with essentially no acid sites present on the surface) (see Table 4). The reactivities of the V_2O_5/SnO_2 and V_2O_5/CeO_2 are 2 orders magnitude higher than that of the V_2O_5/SiO_2, which has been associated with the reducibility of the oxide supports.[42] The presence of a surface SnO_x overlayer between the surface VO_x species and SiO_2 improves the catalytic performance of the V_2O_5/SiO_2 catalyst and increases the methanol oxidation reactivity by 1−2 orders of magnitude relative to that of the V_2O_5/SiO_2 catalyst because of the formation of the VO_x-SnO_x interactions. The presence of bulk CeO_2 particles between the surface VO_x species and SiO_2 increases the methanol oxidation reactivity by 0−1 order of magnitude relative to the V_2O_5/SiO_2 because of the formation of the VO_x-SiO_2 and VO_x-CeO_2 interactions. The formation of the VO_x-SiO_2 and VO_x-CeO_2 interactions in the V_2O_5/CeO_2/SiO_2 catalyst results in lower methanol oxidation reactivity by an order magnitude compared with the reactivity of the V_2O_5/CeO_2 catalysts (see Table 4). Thus, in situ Raman, TPR, and catalytic studies support the conclusion that the specific surface metal oxide−support interactions strongly affect the reactivity and reducibility of the surface vanadium oxide species.[42] The current study demonstrates the capability of molecular design of a supported metal oxide on mixed-oxide support catalysts, and the formation of the specific surface metal oxide−support interactions ensures that the catalysis will be dominated by the surface metal oxide sites.

Conclusions

The molecular structures of V_2O_5 supported on the SnO_2/SiO_2 and CeO_2/SiO_2 mixed oxides during methanol oxidation were monitored by in situ Raman spectroscopy, and the catalytic properties of these catalysts were probed by methanol oxidation. The Raman studies revealed that tin oxide forms a surface SnO_x overlayer on silica surface owing to the absence of Raman features of SnO_2 crystallite, and bulk CeO_2 particles are present on the silica surface. The impregnated vanadium oxide formed a surface vanadia overlayer on all the catalysts owing to the absence of Raman features of V_2O_5 crystallite. In situ Raman studies of the V_2O_5/SnO_2/SiO_2 and V_2O_5/CeO_2/SiO_2 catalysts during methanol oxidation indicate that the formation of the VO_x-SnO_x bonds totally blocks the formation of the surface

$V-OCH_3$ groups, which was only found in the V_2O_5/SiO_2 catalysts. The interaction between the surface VO_x and the surface SnO_x overlayer on silica increases the methanol oxidation reactivity by 1−2 orders of magnitude relative to V_2O_5/SiO_2, and partial interaction between the surface VO_x and bulk CeO_2 particles increases the methanol oxidation reactivity by 0−1 order of magnitude relative to V_2O_5/SiO_2. Temperature programmed reduction (TPR) studies indicate that the reducibility of the surface vanadium oxide species is affected by the reducibility of the specific oxide support, and confirm the formation of the VO_x-SnO_x bonds on the $V_2O_5/SnO_2/SiO_2$ catalyst and the formation of VO_x-CeO_2 as well as VO_x-SiO_2 bonds on the $V_2O_5/CeO_2/SiO_2$ catalyst. Thus, molecular design of a more active supported metal oxide on a mixed-oxide catalyst is related to the specific surface metal oxide−oxygen−support bonds.

Acknowledgment. The financial support of the National Science Council of Taiwan (Grant No. NSC-84-2214-E-005-001) is gratefully acknowledged. The work at Lehigh University is supported by a National Science Foundation (Grant No. CTS-9417981). I especially thank Professor Israel E. Wachs from Lehigh University for the discussions.

References and Notes

(1) Beechman, J. W.; Hegedus, L. L. *Ind. Eng. Chem. Res.* **1991**, *30*, 969.
(2) Boer, F. T.; Hegedus, L. L.; Gouker, T. R.; Zak, K. P. *Chemtech* **1990**, May, 312.
(3) Baiker, A.; Dollenmeier, P.; Glinski, M.; Reller, A. *Appl. Catal.* **1987**, *35*, 365.
(4) Bjorklund, R. B.; Odenbrand, C. U.; Brandin, J. G. M.; Andersson, L. A. H.; Liedberg, B. *J. Catal.* **1989**, *119*, 187.
(5) Rajadhyaksha, R. A.; Hausinger, G.; Zeilinger, H.; Ramsteter, A.; Schmelz, H.; Knozinger, H. *Appl. Catal.* **1989**, *51*, 67.
(6) Bjorklund, R. B.; Jaras, S.; Ackelid, U.; Odenbrand, C. U. I.; Andersson, L. A. H.; Brandin, J. G. M. *J. Catal.* **1991**, *128*, 574.
(7) Wauthoz, P.; Ruwet, M.; Machej, T.; Grange P. *Appl. Catal.* **1991**, *69*, 149.
(8) Jehng, J. M.; Wachs, I. E. *Catal. Lett.* **1992**, *13*, 9.
(9) Deo, G.; Wachs, I. E. *J. Catal.* **1991**, *129*, 137.
(10) Okada, F.; Satsuma, A.; Furnta, A.; Miyamoto, A.; Hattori, T.; Murakami, Y. *J. Phys. Chem.* **1990**, *94*, 5900.
(11) Reddy, B. M. In *Catalytic Selective Oxidation*; ACS Symposium Series; American Chemical Society: Washington, DC, 1993; Vol. 523, p 204.
(12) Sobalik, Z.; Lapina, O. B.; Novogorodova, O. N.; Mastikhin, V. M. *Appl. Catal.* **1990**, *63*, 191.
(13) Narsimha, K.; Reddy, B. M.; Rao, P. K.; Mastikhin, V. M. *J. Phys. Chem.* **1990**, *94*, 7336.
(14) Chary, K. V. R.; Reddy, B. M.; Nag, N. K.; Subrahmanyam, V. S.; Sunandana, C. S. *J. Phys. Chem.* **1984**, *88*, 2622.
(15) Cavani, F.; Centi, G.; Foresti, E.; Trifiro, F. *J. Chem. Soc., Faraday Trans.* **1988**, *84*, 237.
(16) Qun, S.; Jehng, J. M.; Hu, H.; Herman, R. G.; Wachs, I. E.; Klier, K. *J. Catal.* **1997**, *165*, 91.
(17) Ramis, G.; Cristiani, C.; Forzatti, P.; Busca, G. *J. Catal.* **1990**, *124*, 574.
(18) Bond, G. C. *Appl. Catal.* **1991**, *71*, 1.
(19) Bond, G. C.; Vedrine, J. C. *Catal. Today* **1994**, 20 (special issue).
(20) Das, N.; Eckert, H.; Hu, H.; Wachs, I. E.; Walzer, J. F.; Feher, F. J. *J. Phys. Chem.* **1993**, *97*, 8240.
(21) Eckert, H.; Wachs, I. E. *J. Phys. Chem.* **1989**, *93*, 6796.
(22) Hanuza, J.; Jezowska-Trzebiatowska, B.; Oganowski, W. *J. Mol. Catal.* **1985**, *29*, 109.
(23) Yoshida, S.; Tanaka, T.; Nishiumura, Y.; Mizutani, H.; Funabiki, T. *Proc. Int. Congr. Catal., 9th* **1988**, *3*, 1473.
(24) Vuurman, M.; Wachs, I. E.; Hirt, A. M. *J. Phys. Chem.* **1991**, *95*, 9928.
(25) Deo, G.; Eckert, H.; Wachs, I. E. *Prepr.—Am. Chem. Soc., Div. Pet. Chem.* **1990**, *35* (1), 16.
(26) Went, G. T.; Oyama, S. T.; Bell, A. T. *J. Phys. Chem.* **1990**, *94*, 4240.
(27) Oyama, S. T.; Went, G. T.; Lewis, K. B.; Bell, A. T.; Somarjai, G. *J. Phys. Chem.* **1989**, *93*, 6786.
(28) Reedy, B. M.; Narsimha, K.; Sivaraj, C.; Rao, P. *Appl. Catal.* **1989**, *55*, 11.
(29) Cristinai, C.; Forzatti, P.; Busca, G. *J. Catal.* **1989**, *116*, 586.
(30) Went, G. T.; Oyama, S. T. *J. Phys. Chem.* **1990**, *94*, 4240.
(31) Deo, G.; Hardcastle, F. D.; Richards, M.; Wachs, I. E.; Hirt, A. M. In *Novel Materials in Heterogeneous Catalysis*; Baker, R. T., Murrell, L. L., Eds.; ACS Symposium Series; American Chemical Society: Washington, DC, 1990; Vol. 437, p 317.
(32) Jehng, J. M.; Hu, H.; Gao, X.; Wachs, I. E. *Catal. Today*. **1996**, *28*, 337.
(33) Busca, G.; Elmi, A. S.; Forzatti, P. *J. Phys. Chem.* **1987**, *91*, 5263.
(34) Tatibouet, J. M. *Appl. Catal. A* **1997**, *148*, 213.
(35) Hardcastle, F. D.; Wachs, I. E. *J. Phys. Chem.* **1991**, *95*, 5031.
(36) Busca, G. *Mater. Chem. Phys.* **1988**, *19*, 157.
(37) Davydov, A. A. *Kinet. Katal.* **1993**, *34*, 951.
(38) Andersson, A. *J. Catal.* **1981**, *69*, 465.
(39) Anderson, M. W.; Suib, S. I.; Occelli, M. L. *J. Mol. Catal.* **1990**, *61*, 295.
(40) Lide, D. R., Ed. *CRC Handbook of Chemistry and Physics*, 75th ed.; CRC Press: Boca Raton, FL, 1995; Chapter 4, p 148.
(41) Wachs, I. E.; Weckhuysen, B. M. *Appl. Catal. A* **1997**, *3788*, 1.
(42) Deo, G.; Wachs, I. E. *J. Catal.* **1994**, *146*, 323.
(43) Roozeboom, F.; Mitelmeijer-Hazeleger, M. C.; Moulijn, J. A.; Medema, J.; de Beer, V. H. J.; Gellings, P. J. *J. Phys. Chem.* **1980**, *84*, 2783.
(44) Nickel, J.; Dutroit, D.; Baiker, A.; Scharf, U.; Wokaun, A. *Ber. Bunsen-Ges. Phys. Chem.* **1993**, *97*, 217.
(45) Kijenski, K.; Baiker, A.; Glinski, M.; Dollenmeier, P.; Wokaun, A. *J. Catal.* **1986**, *101*, 1.
(46) Haber, J.; kozlowska, A.; kozlowsi, R. *J. Catal.* **1986**, *102*, 52.
(47) Koranne, M. M.; Goodwin, J. G.; Marcelin, G. Jr. *J. Catal.* **1994**, *148*, 369.
(48) Went, G. T.; Leu, L.-J.; Bell, A. T. *J. Catal.* **1992**, *134*, 479.
(49) Went, G. T.; Leu, L.-J.; Rosin, R. R.; Bell, A. T. *J. Catal.* **1992**, *134*, 492.
(50) Weckhuysen, B. M.; Wachs, I. E. *J. Phys. Chem.* **1996**, *100*, 14437.